Anomalous Thermal Conductivity and Magnetic Torque Response in the Honeycomb Magnet α-$RuCl_3$

Ian A. Leahy,[1] Christopher A. Pocs,[1] Peter E. Siegfried,[1] David Graf,[2] S.-H. Do,[3] Kwang-Yong Choi,[3] B. Normand,[4] and Minhyea Lee[1]

[1]*Department of Physics, University of Colorado, Boulder, Colorado 80309, USA*
[2]*National High Magnetic Field Laboratory, Tallahassee, Florida 32310, USA*
[3]*Department of Physics, Chung-Ang University, Seoul 790-784, South Korea*
[4]*Laboratory for Neutron Scattering and Imaging, Paul Scherrer Institute, CH-5232 Villigen PSI, Switzerland*

(Received 28 December 2016; published 5 May 2017)

We report on the unusual behavior of the in-plane thermal conductivity κ and torque τ response in the Kitaev-Heisenberg material α-$RuCl_3$. κ shows a striking enhancement with linear growth beyond $H = 7$ T, where magnetic order disappears, while τ for both of the in-plane symmetry directions shows an anomaly at the same field. The temperature and field dependence of κ are far more complex than conventional phonon and magnon contributions, and require us to invoke the presence of unconventional spin excitations whose properties are characteristic of a field-induced spin-liquid phase related to the enigmatic physics of the Kitaev model in an applied magnetic field.

DOI: 10.1103/PhysRevLett.118.187203

Low-dimensional spin systems display a multitude of quantum phenomena, providing an excellent forum for the exploration of unconventional ground states and their exotic excitations. The Kitaev model [1] has attracted particular attention, both theoretically and experimentally, because it possesses an exactly solvable quantum spin-liquid (QSL) ground state and has possible realizations in a number of candidate materials [2–5]. Thermal transport measurements have proven to be a powerful tool for elucidating the itinerant nature of QSLs [6,7], as a result of their high sensitivity to the low-energy excitation spectrum, and in fact studies of low-dimensional insulating quantum magnets have revealed very significant contributions to heat conduction from unconventional spin excitations [8–18].

Magnetic insulators containing $4d$ and $5d$ elements combine electronic correlation effects with strong spin-orbit coupling (SOC) to generate complex magnetic interactions. In the Kitaev model, nearest-neighbor spin-$\frac{1}{2}$ entities on a two-dimensional (2D) honeycomb lattice interact through a bond-dependent Ising-type coupling of different spin components, whose strong frustration leads to a QSL ground state with emergent gapless and gapped Majorana-fermion excitations [1]. The physical realization of this uniquely anisotropic interaction requires strong SOC, which creates effective $j_{\rm eff} = \frac{1}{2}$ moments with Kitaev-type coupling in the honeycomb iridate compounds A_2IrO_3 (A = Na or Li) [19,20]. Despite its weaker SOC, the $4d$ honeycomb material α-$RuCl_3$ contains similar spin-orbit-entangled moments, and thus has emerged as another candidate system for Kitaev-related physics [5,21–23].

In this Letter, we present in-plane thermal conductivity κ and magnetic torque τ studies of single-crystal α-$RuCl_3$ samples. Below the magnetic ordering temperature T_C a pronounced minimum of κ and an accompanying torque anomaly at $H = H_{\rm min} \simeq 7$ T occur due to a field-induced phase transition from the "zig-zag" ordered state [21,24] to a spin-disordered phase. The abrupt and linear rise of the low-T κ at $H > H_{\rm min}$ indicates that this field-induced spin liquid (FISL) contains a massless excitation with Dirac-type dispersion, while the strong renormalization of the phonon contribution at all temperatures suggests a broad band of unconventional medium-energy excitations. These results serve to fingerprint the possible Kitaev physics of the FISL in α-$RuCl_3$.

Single crystals of $RuCl_3$ were synthesized by vacuum sublimation [25], as described in Sec. SI of the Supplemental Material (SM) [26]. κ measurements were performed with a one-heater, two-thermometer configuration in a ^{3}He refrigerator and external magnetic fields up to 14 T. Cernox and RuO_x resistors were used as thermometers for the respective temperature ranges $T > 2$ K and $0.3 < T \leq 15$ K, and were calibrated both separately and *in situ* under the applied field. Both the thermal current ($-\nabla T$) and the field were oriented in the crystalline ab plane, with H applied either parallel or perpendicular to ∇T. We found little difference in κ for the two orientations, and all results shown below were measured in the $\nabla T \| H \| ab$ geometry, other than Fig. 1(b), where $\nabla T \perp H$. τ was determined from capacitance measurements between the ground plane and a BeCu cantilever. Its angular dependence was measured in two geometries, one in which H was rotated within the ab plane (ϕ rotation) and one with H rotated out of plane (θ rotation).

Figure 1(a) shows $\kappa(T)$, in fields $\mu_0 H = 0$ and 14 T, for three α-$RuCl_3$ samples. Qualitatively, the dependence of κ

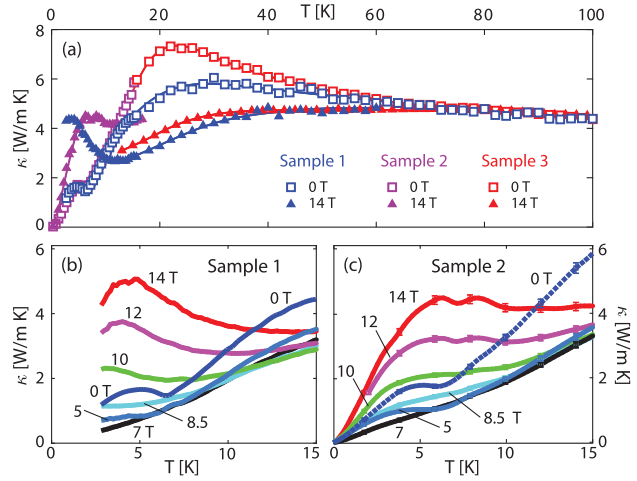

FIG. 1. (a) In-plane thermal conductivity $\kappa(T)$ shown up to 100 K for Samples 1, 2, and 3 at $\mu_0 H = 0$ T (squares) and 14 T (triangles). The solid lines are a guide to the eye. (b) Low-temperature detail of $\kappa(T)$ for a range of H values, shown for Sample 1. (c) $\kappa(T)$ at low T for Sample 2.

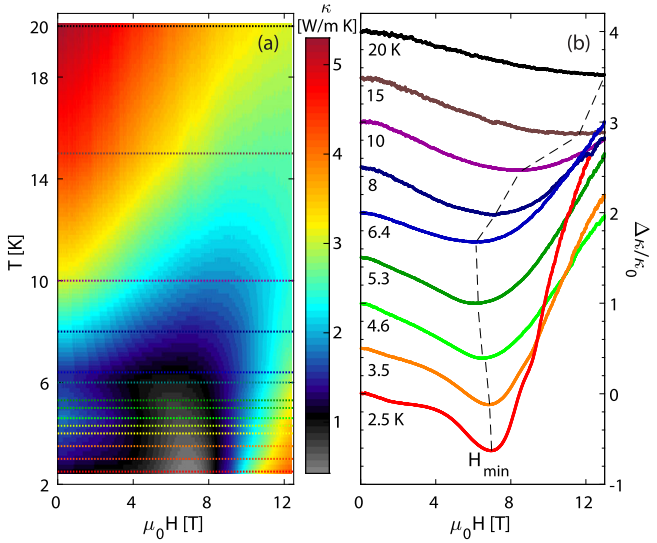

FIG. 2. (a) $\kappa(T, H)$ for Sample 1, represented by color contours. The horizontal lines correspond to field sweeps measuring $\kappa(H)$ at fixed T. (b) Relative thermal conductivity difference $\Delta\kappa(H)/\kappa_0$ shown for the fixed values of T highlighted in panel (a); the curves are presented with constant offsets.

on both T and H is the same in each case, and we focus on these general features. Quantitatively, our samples show differences in peak heights and widths, which we relate to their age and defect content in Sec. SI of the SM [26]. On cooling at zero field (ZF), $\kappa_0(T) = \kappa(T, H = 0)$ has a broad peak near 25 K and decreases down to the magnetic ordering temperature $T_C \simeq 6.3$ K, which is identified both from the upturn in κ and from the magnetic susceptibility (data not shown). This value of T_C is identified clearly in all our crystals, testifying to their high as-grown quality, with no contamination from structures of different layer stackings [27]. For $T < T_C$, $\kappa_0(T)$ shows a weak maximum before decreasing to zero. $\kappa(T, 14\ \mathrm{T})$ differs dramatically from $\kappa_0(T)$ at all temperatures below 60 K. Its peak at intermediate T is suppressed, broader, and lies at a higher temperature, whereas below $T \simeq 12$ K it has a strong low-T peak that is completely absent from $\kappa_0(T)$.

Focusing on this low-T regime, Figs. 1(b) and 1(c) show $\kappa(T)$ at constant fields $H = 0$, 5, 7, 8.5, 10, 12, and 14 T. Because the ordered state has a large magnon gap [28], the weak low-T, low-H feature is in fact an enhanced phonon contribution. This is suppressed with increasing field, and the minimum marking T_C is visible up to $H = 5$ T. At $H = H_{\mathrm{min}} \simeq 7$ T, both the phonon enhancement and the minimum disappear. Further increase of H causes the appearance of the low-T peak, whose height grows linearly with $H - H_{\mathrm{min}}$, leading to rounded maxima around 5 K at 14 T. We have collected detailed low-T data ($0.3 < T < 3$ K) at $H > H_{\mathrm{min}}$ for Sample 2 [Fig. 1(c)] and find that these do not display an activated form; the alternative of a power-law form demonstrates clearly that this feature is the contribution of a gapless excitation.

The nonmonotonic evolution with H and the strong high-field enhancement of κ are clearly evident in the isothermal H dependence. Figure 2(a) presents $\kappa(H, T)$ for Sample 1 as a color contour map, showing the minimum region around H_{min} and maxima at high T or high H. The fractional change of $\kappa(H)$, $\Delta\kappa/\kappa_0 = (\kappa(H) - \kappa_0)/\kappa_0$, is shown in Fig. 2(b) for a range of T values. $\kappa(H)$ and $\Delta\kappa(H)/\kappa_0$ show an initial decrease, before turning over at H_{min} and increasing rapidly. $H_{\mathrm{min}}(T)$ remains around 7 T for $T < T_C$, but becomes rapidly larger as T is increased beyond T_C, making the minima shallower until at $T = 20$ K H_{min} is pushed outside our measurement range. Our measured value $H_{\mathrm{min}} \simeq 7$ T for $T < 10$ K coincides with the critical field (H_C) for the field-induced phase transition observed in bulk magnetization [24] and specific-heat measurements [29]. Further, the magnetization in this field range is far from saturation [24,29] and it is safe to conclude that the system is only weakly spin polarized above H_{min}.

In general, κ contains multiple terms whose effects can be difficult to separate. For α-$RuCl_3$, the presence and location of H_{min} are fundamental properties of the phase diagram and four further, distinctive features provide clues about the primary contributions to κ. These are (i) the local minimum in $\kappa(T)$ occurring at T_C at small H [Figs. 1(b) and 1(c)], (ii) the slow decrease of $\kappa(H)$ when H increases from zero [Fig. 2(b)], (iii) the properties of the low-T peak in $\kappa(T)$ at $H > H_{\mathrm{min}}$ [Figs. 1(b) and 1(c)], and (iv) the suppression and shift of the intermediate-temperature contribution by the applied field [Fig. 1(a)].

Features (i) and (ii) can be explained within a conventional framework. The magnetic anisotropy of $RuCl_3$

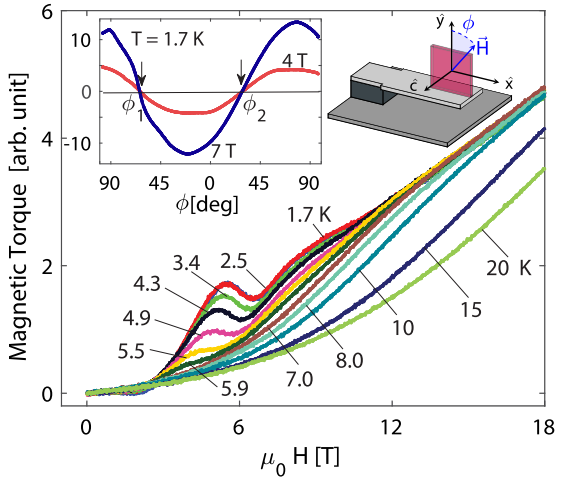

FIG. 3. In-plane torque response as a function of H, measured at selected values of T with $\phi = -69° \pm 2°$. Right inset: measurement configuration. Left inset: ϕ dependence of τ at fields of 4 and 7 T; $\phi_1 = -64°$ and $\phi_2 = 28°$ exhibit 90° symmetry ($\phi = 0°$ is chosen arbitrarily).

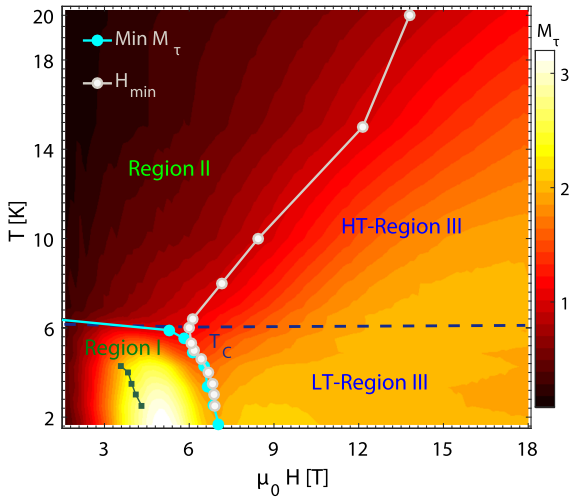

FIG. 4. (a) (H, T) phase diagram of α-$RuCl_3$ inferred from the magnitude of M_τ measured at $\phi \simeq -69°$ (color scale). The white circles indicate $H_{\min}$ as a function of T, the cyan circles indicate the position of local minima in $M_\tau(H)$, and the green squares indicate the locations of inflection points appearing in $\Delta\kappa/\kappa_0(H)$ [Fig. 2(b)].

results in a magnon gap of 1.7 meV [28] in the ordered state, and thus no spin-wave contribution can be expected. In many systems, κ decreases rapidly below the Curie-Weiss temperature $T_{\rm CW}$ due to the scattering of phonons by spin fluctuations, which reduces the phonon mean free path l_p. Such spin-phonon scattering is thought to have a strong impact on the phonon contribution to heat conduction in SOC materials [30,31]. In $RuCl_3$, this effect is visible below $T_{\rm CW} \approx 25$ K [21] at ZF [Fig. 1(a)]. However, spin fluctuations are suppressed due to the onset of magnetic order, i.e., below $T = T_C$. Thus, the weak low-T, low-H feature, whose vanishing causes the pronounced local minimum at T_C in ZF (i), is caused by the enhancement of κ expected from the improved l_p. By the same token, the weak decrease of κ with T for $H < H_{\min}$ (ii) is a consequence of the applied field suppressing the magnetic order, and with it the improved l_p.

Before discussing features (iii) and (iv), for further perspective concerning the phases below and above $H_{\min}$ we have performed magnetic torque measurements on our $RuCl_3$ single crystals. We rotate H both within the ab plane (Fig. 3, right inset) and out of it (discussed in Sec. SII of the SM [26]). The torque generated in the presence of a magnetization $\mathbf{M}$ is $\boldsymbol{\tau} = \mu_0 \mathbf{M} V \times \mathbf{H}$, with μ_0 the permeability and V the sample volume. The thermodynamic quantity τ is highly sensitive to magnetic anisotropy [32,33]. Measurements performed on three crystals, of different shapes and sizes, all returned results very similar to those shown in Fig. 3.

In the ab plane, $\tau(\phi)$ displays the 90° symmetry expected due to the monoclinic structure of α-$RuCl_3$ [25,27] (Fig. 3, left inset). At two specific angles, ϕ_1 and ϕ_2, $\tau \to 0$ independent of the magnitude of H, and Fig. 3 shows $\tau(H)$ measured near ϕ_1 (results near ϕ_2 are qualitatively similar). At low T, $\tau(H)$ with $H < H_{\min}$ exhibits a strikingly nonmonotonic form. This complexity ceases abruptly at $H > H_{\min}$. At $T > T_C$, the sizes both of τ and of the anomaly drop significantly, indicating strongly that this behavior is due solely to the presence of magnetic order. Such anomalous H dependence is not surprising in a Hamiltonian as anisotropic as the Kitaev-Heisenberg model, and a rich variety of complex field-induced ordering patterns, with corresponding off-diagonal components of the magnetic susceptibility tensor, has been suggested [34,35].

We define the torque magnetization $M_\tau = \tau/H$, which in certain geometries is closely related to the real magnetization (as discussed in Sec. III of the SM [26]). Figure 4 shows $M_\tau(H, T)$ in the form of color contours [36]. The overlaid points showing the characteristic quantities $H_{\min}(T)$ and the minima of M_τ divide this effective H-T phase diagram naturally into three distinct regions. Region I, at $T < T_C$ and $H < H_{\min}$, is where spontaneous magnetic order exists and is characterized by the strongly nonmonotonic $\tau(H)$ and decreasing $\kappa(H)$ ($d\kappa/dH < 0$). Here also the inflection points of $\kappa(H)$ at $H < H_{\min}$ [Fig. 4(a)] coincide with the local maxima of τ (Fig. 3). In Region II, $d\kappa/dH < 0$ while $T > T_C$. Region III is characterized by $d\kappa/dH > 0$, but the derivative falls rapidly as T crosses T_C, leading us to divide it into low-temperature (LT)–Region III ($T < T_C$), where we observe the strongest enhancement of $\Delta\kappa/\kappa_0$, and high-temperature (HT)–Region III ($T > T_C$), where $H_{\min}$ moves rapidly to higher values.

Features (iii) and (iv) in κ are, respectively, the key properties of Regions LT–III and HT–III. Before invoking exotic physics, the conventional explanations should be exhausted. Modeling all the contributions of phonons and

coherent spin excitations to κ is a complicated problem [8–15,17,18]. The first complexity for α-$RuCl_3$ is the quasi-2D structure, which would require a currently unavailable anisotropic 3D phonon fit. Conventional phonon thermal conductivity in a magnetic insulator is ascribed to four contributions: point defects, grain boundaries, umklapp processes, and magnon-phonon resonant scattering [37–39]. The last has been used successfully to describe the H dependence of features observed in κ in several low-dimensional materials [10,40,41]. However, its effect is usually to generate a minimum at the resonance energy, causing a double-peak structure in $\kappa(T)$ where only the lower peak has strong H dependence [8,10,41]. Such behavior is qualitatively different from α-$RuCl_3$, and in fact we are not aware of a mechanism for a strong field-induced enhancement of κ, of the type we observe in Figs. 1(b) and 1(c), other than a coherent spin excitation [12–14,16,42]. However, α-$RuCl_3$ at $H > H_{\mathrm{min}}$ has no magnetic order, as demonstrated by the absence of features in the susceptibility [21] and specific heat [29], and verified by neutron scattering [43] and nuclear magnetic resonance studies [44]. Thus, it has no conventional gapless mode, and this is why we conclude that feature (iii) must be attributed to an unconventional excitation of the FISL.

Turning to exotic solutions, the proximity of the zig-zag ordered state to a Kitaev QSL at ZF [22] is strongly suggestive. However, we note that an applied field destroys many of the exotic properties of the Kitaev QSL [1], that the FISL is partially spin polarized, that the Heisenberg terms have nontrivial effects [22], and that ideal honeycomb symmetry is broken in monoclinic α-$RuCl_3$ [27,45]. It is nevertheless instructive to recall that the Kitaev model has an exact solution in terms of Majorana fermions, one of which is massless with linear dispersion [1] while the others are massive. Spin excitations are Majorana pairs, or equivalently Majorana modes pinned to static fluxes [46], and are all massive. Although one recent numerical study reports a QSL state above a critical field in a model for $RuCl_3$ [47], it was found to be gapped. The low- and medium-energy spin excitations of $RuCl_3$ at ZF have been mapped by recent inelastic neutron scattering studies [28,48]. In addition to the gapped spin waves, one finds a broad continuum of excitations centered around 5 meV [48]. At finite fields, no unambiguous information is yet available, other than the κ signals we measure. For their interpretation, it is of crucial importance that the low-T excitations contributing to κ above H_{min} are gapless and that their density of states increases linearly with H [feature (iii)]. These are the properties of a cone-type dispersion and are thus the same behavior as the massless Kitaev QSL mode.

Feature (iv) is the striking field dependence of $\kappa(T)$ for $T_C < T < 60$ K [Fig. 1(a)]. In this range κ should be dominated by phonons, whose contributions are H independent. The presence of an incoherent medium-energy continuum of anisotropic spin excitations [48] may cause a direct contribution to κ or a suppression due to spin-phonon scattering. Our results contain no evidence for direct contributions, as there is no abrupt change in κ at H_{min} and the change in the high-T peak position indicates energy shifts far beyond the scale of H. By contrast, our results contain several features characterizing a strong suppression of phonon contributions. First, κ at ZF cannot be fitted within the conventional framework, indicating that anomalous phonon scattering is significant even at $H = 0$. Second, the continuum affects the phonon contributions to κ over a broad range of T [Fig. 1(a)], reflecting the broad energy range observed in Ref. [48]. Third, scattering becomes considerably more effective at a field of 14 T. Because the field scale for a significant reconstruction of the continuum should be the Kitaev energy, estimated as $K \approx 7$ meV [23,28], it is clear that some rearrangement must take place at the field-induced transition to the FISL. However, the lack of abrupt changes in κ at H_{min} indicates that only a small fraction of the continuum turns into the massless mode [feature (iii)], while the majority of its spectral weight remains in a broad continuum at finite energies; we comment here that thermal fluctuations may cause at least as strong a rearrangement of the continuum over the T range of our experiment as field effects do. Thus, from the evidence provided by $\kappa(H, T)$, the FISL does appear to possess both the primary excitation features of the Kitaev QSL, namely a Dirac-type band and a finite-energy continuum. For this reason we refer to them as proximate Kitaev excitations (PKEs).

To summarize the nature of heat conduction in α-$RuCl_3$ in the context of Fig. 4, κ in Region I is controlled by low-T phonon contributions, decreasing slowly as the system is driven towards the FISL because l_p is reduced. A similar trend continues in Region II, where the increasing thermal population of phonons, as well as thermally excited paramagnons, contribute to κ. In LT–Region III, the rapid increase of κ with H reflects the presence of the massless PKE. In HT–Region III, the minimum of $\kappa(H)$ moves to high fields (Fig. 4) and there are contributions to κ both from phonons and from the massive PKEs, where the primary effect of the latter is the systematic suppression of the former with increasing H, which drives up the crossover field $[H_{\mathrm{min}}(T)]$ from Region II.

To conclude, we have investigated the highly nonmonotonic thermal conductivity and the torque magnetization response of the 2D honeycomb-lattice material $RuCl_3$. We infer a field-induced phase transition to a state, the FISL, of no magnetic order and no simple spin polarization. The low-energy excitations of this spin-disordered ground state cause a dramatic enhancement of κ at low temperatures, while its gapped excitations suppress the phonon contribution at higher temperatures, and do so more effectively at higher fields. Although our results neither prove nor disprove that the FISL is closely related to the Kitaev QSL state, they set strong constraints on the nature of its excitations and thus of its theoretical description.

We thank A. Chernyshev and M. Hermele for helpful discussions. This work was supported by the U.S. DOE, Basic Energy Sciences, Materials Sciences and Engineering Division, under Award No. DE-SC0006888. Torque magnetometry was performed at the National High Magnetic Field Laboratory, which is supported by National Science Foundation Cooperative Agreement No. DMR-1157490 and the State of Florida. S.-H. D. and K.-W. C. were supported by the National Research Foundation of Korea through Grants No. 2009-0093817 and No. 20160540.

[1] A. Kitaev, Ann. Phys. (Amsterdam) **321**, 2 (2006).
[2] G. Jackeli and G. Khaliullin, Phys. Rev. Lett. **102**, 017205 (2009).
[3] J. Chaloupka, G. Jackeli, and G. Khaliullin, Phys. Rev. Lett. **105**, 027204 (2010).
[4] Y. Singh, S. Manni, J. Reuther, T. Berlijn, R. Thomale, W. Ku, S. Trebst, and P. Gegenwart, Phys. Rev. Lett. **108**, 127203 (2012).
[5] K. W. Plumb, J. P. Clancy, L. J. Sandilands, V. V. Shankar, Y. F. Hu, K. S. Burch, H.-Y. Kee, and Y.-J. Kim, Phys. Rev. B **90**, 041112 (2014).
[6] M. Yamashita, N. Nakata, Y. Kasahara, T. Sasaki, N. Yoneyama, N. Kobayashi, S. Fujimoto, T. Shibauchi, and Y. Matsuda, Nat. Phys. **5**, 44 (2009).
[7] M. Yamashita, N. Nakata, Y. Senshu, M. Nagata, H. M. Yamamoto, R. Kato, T. Shibauchi, and Y. Matsuda, Science **328**, 1246 (2010).
[8] Y. Ando, J. Takeya, D. L. Sisson, S. G. Doettinger, I. Tanaka, R. S. Feigelson, and A. Kapitulnik, Phys. Rev. B **58**, R2913 (1998).
[9] A. V. Sologubenko, K. Giannó, H. R. Ott, U. Ammerahl, and A. Revcolevschi, Phys. Rev. Lett. **84**, 2714 (2000).
[10] M. Hofmann, T. Lorenz, G. S. Uhrig, H. Kierspel, O. Zabara, A. Freimuth, H. Kageyama, and Y. Ueda, Phys. Rev. Lett. **87**, 047202 (2001).
[11] A. V. Sologubenko, K. Gianno, H. R. Ott, A. Vietkine, and A. Revcolevschi, Phys. Rev. B **64**, 054412 (2001).
[12] B. C. Sales, M. D. Lumsden, S. E. Nagler, D. Mandrus, and R. Jin, Phys. Rev. Lett. **88**, 095901 (2002).
[13] R. Jin, Y. Onose, Y. Tokura, D. Mandrus, P. Dai, and B. C. Sales, Phys. Rev. Lett. **91**, 146601 (2003).
[14] S. Y. Li, L. Taillefer, C. H. Wang, and X. H. Chen, Phys. Rev. Lett. **95**, 156603 (2005).
[15] C. Hess, Eur. Phys. J. Spec. Top. **151**, 73 (2007).
[16] X. F. Sun, W. Tao, X. M. Wang, and C. Fan, Phys. Rev. Lett. **102**, 167202 (2009).
[17] L. M. Chen, X. M. Wang, W. P. Ke, Z. Y. Zhao, X. G. Liu, C. Fan, Q. J. Li, X. Zhao, and X. F. Sun, Phys. Rev. B **84**, 134429 (2011).
[18] A. Mohan, N. S. Beesetty, N. Hlubek, R. Saint-Martin, A. Revcolevschi, B. Büchner, and C. Hess, Phys. Rev. B **89**, 104302 (2014).
[19] S. K. Choi, R. Coldea, A. N. Kolmogorov, T. Lancaster, I. I. Mazin, S. J. Blundell, P. G. Radaelli, Y. Singh, P. Gegenwart, K. R. Choi, S.-W. Cheong, P. J. Baker, C. Stock, and J. Taylor, Phys. Rev. Lett. **108**, 127204 (2012).
[20] S. H. Chun, J.-W. Kim, J. Kim, H. Zheng, C. C. Stoumpos, C. D. Malliakas, J. F. Mitchell, K. Mehlawat, Y. Singh, Y. Choi, T. Gog, A. Al-Zein, M. Sala, M. Krisch, J. Chaloupka, G. Jackeli, G. Khaliullin, and B. J. Kim, Nat. Phys. **11**, 462 (2015).
[21] J. A. Sears, M. Songvilay, K. W. Plumb, J. P. Clancy, Y. Qiu, Y. Zhao, D. Parshall, and Y.-J. Kim, Phys. Rev. B **91**, 144420 (2015).
[22] J. G. Rau, E. K.-H. Lee, and H.-Y. Kee, Phys. Rev. Lett. **112**, 077204 (2014).
[23] H.-S. Kim, V. Vijay Shankar, A. Catuneanu, and H.-Y. Kee, Phys. Rev. B **91**, 241110 (2015).
[24] R. D. Johnson, S. C. Williams, A. A. Haghighirad, J. Singleton, V. Zapf, P. Manuel, I. I. Mazin, Y. Li, H. O. Jeschke, R. Valentí, and R. Coldea, Phys. Rev. B **92**, 235119 (2015).
[25] S.-Y. Park, S.-H. Do, K.-Y. Choi, D. Jang, T.-H. Jang, J. Schefer, C.-M. Wu, J. S. Gardner, J. M. S. Park, J.-H. Park, and S. Ji, arXiv:1609.05690.
[26] See Supplemental Material at http://link.aps.org/supplemental/10.1103/PhysRevLett.118.187203 for details.
[27] H. B. Cao, A. Banerjee, J.-Q. Yan, C. A. Bridges, M. D. Lumsden, D. G. Mandrus, D. A. Tennant, B. C. Chakoumakos, and S. E. Nagler, Phys. Rev. B **93**, 134423 (2016).
[28] A. Banerjee, C. A. Bridges, J.-Q. Yan, A. A. Aczel, L. Li, M. B. Stone, G. E. Granroth, M. D. Lumsden, Y. Yiu, J. Knolle, D. L. Kovrizhin, S. Bhattacharjee, D. A. Tennant, R. Moessner, D. G. Mandrus, and S. E. Nagler, Nat. Mater. **15**, 733 (2016).
[29] Y. Kubota, H. Tanaka, T. Ono, Y. Narumi, and K. Kindo, Phys. Rev. B **91**, 094422 (2015).
[30] F. Steckel, A. Matsumoto, T. Takayama, H. Takagi, B. Büchner, and C. Hess, Europhys. Lett. **114**, 57007 (2016).
[31] A. L. Chernyshev, Phys. Rev. B **72**, 174414 (2005).
[32] R. Okazaki, T. Shibauchi, H. J. Shi, Y. Haga, T. D. Matsuda, E. Yamamoto, Y. Onuki, H. Ikeda, and Y. Matsuda, Science **331**, 439 (2011).
[33] S. Kasahara, H. J. Shi, K. Hashimoto, S. Tonegawa, Y. Mizukami, T. Shibauchi, K. Sugimoto, T. Fukuda, T. Terashima, A. H. Nevidomskyy, and Y. Matsuda, Nature (London) **486**, 382 (2012).
[34] L. Janssen, E. C. Andrade, and M. Vojta, Phys. Rev. Lett. **117**, 277202 (2016).
[35] G.-W. Chern, Y. Sizyuk, C. Price, and N. B. Perkins, arXiv:1611.03436.
[36] Figure S3 of the SM [26] shows the corresponding curves for $M_\tau(H)$ at different values of T.
[37] P. Klemens, *Solid State Physics* (Academic Press, New York, 1958), Vol. 7.
[38] J. Callaway, Phys. Rev. **113**, 1046 (1959).
[39] R. Berman, *Thermal Conduction in Solids* (Oxford University Press, Oxford, 1979).
[40] J. C. Wu, J. D. Song, Z. Y. Zhao, J. Shi, H. S. Xu, J. Y. Zhao, X. G. Liu, X. Zhao, and X. F. Sun, J. Phys. Condens. Matter **28**, 056002 (2016).
[41] B.-G. Jeon, B. Koteswararao, C. B. Park, G. J. Shu, S. C. Riggs, E. G. Moon, S. B. Chung, F. C. Chou, and K. H. Kim, Sci. Rep. **6**, 36970 (2010).

[42] X. M. Wang, C. Fan, Z. Y. Zhao, W. Tao, X. G. Liu, W. P. Ke, X. Zhao, and X. F. Sun, Phys. Rev. B **82**, 094405 (2010).
[43] S. E. Nagler (private communication).
[44] S.-H. Baek, S.-H. Do, K.-Y. Choi, Y. S. Kwon, A. U. B. Wolter, J. van den Brink, and B. Büchner, arXiv:1702.01671.
[45] H.-S. Kim and H.-Y. Kee, Phys. Rev. B **93**, 155143 (2016).
[46] G. Baskaran, S. Mandal, and R. Shankar, Phys. Rev. Lett. **98**, 247201 (2007).
[47] R. Yadav, N. A. Bogdanov, V. M. Katukuri, S. Nishimoto, J. van den Brink, and L. Hozoi, Sci. Rep. **6**, 37925 (2016).
[48] A. Banerjee, J.-Q. Yan, J. Knolle, C. A. Bridges, M. B. Stone, M. D. Lumsden, D. G. Mandrus, D. A. Tennant, R. Moessner, and S. E. Nagler, arXiv:1609.00103.